A Comparison of Formulations of the Volatility Surface

Student Number: 01389888
August 2, 2018

Imperial College Business School
MSc Risk Management & Financial Engineering

Abstract

The advantages and drawbacks of the LMM, SABR and a non-parametric swaption volatility model are discussed with regards to the construction of the swaption volatility cube in an industry setting.

Contents

List of Figures

Note that images of all volatility surfaces for all models are available through the interactive online appendix found at: https://01389888.github.io/AP/.

List of Tables

Project Specification

A global hedge fund is in the process of expanding it's trading operations into the fixed income sector to implement a variety of proprietary strategies trading swaptions in particular. A number of the funds current and potential investors have expressed concern that the fund will be trading far more exotic and less transparent products than previously. The fund believes that by showcasing a variety of the more prominent and recent models it intends to use to manage and mark-to-market their swaptions books, the concerned investors will be more comfortable with its expansion.

The aim of the report is to:

- give an overview of the Libor Market Model which the fund may use to verify and calibrate it's forward curve to the swaptions market and display awareness of its drawbacks
- give a more detailed explanation of the SABR model that the fund intends to use primarily to value manage it's swaptions book and provide intuitive explanations of it's key features
- show an example of the most current progressive research in the area that is likely to be implemented in the valuing of the more exotic products as it advances in the near future.

Alongside the report to be distributed, the fund has also created an interactive platform through which the investors can view and interact with the models that are calibrated to recent market data. This platform can be found at: https://01389888.github.io/AP/.

Introduction

The option volatility surface is a well-known and extensively researched area of quantitative finance. It is formed using the option maturity T, the option's strike K, and some measure of the option's volatility. Following the introduction of the Black-Scholes option pricing formula, the implied volatility as given by this formula has been the measure used to quote option prices in the market (Hagan et al., 2002). However, the assumption in the Black-Scholes model of constant volatility is incorrect and so the implied volatility is unable to accommodate volatility smiles and skews observed in the market and is insufficient in the pricing of more exotic derivatives. As a result, a variety of models have been developed aiming to calibrate a volatility surface to market prices under the assumption that they are arbitrage free. These models include the non-parametric local volatility model developed by Dupire, Derman and Kani in 1994 where they show that under risk neutrality, there is a unique diffusion process consistent with the distribution of the underlying. Such a local volatility model aids in the pricing of illiquid and exotic derivatives (Gatarek, Jablecki, 2017). Other prominent models include the Jump-Diffusion model (Merton, 1976) and the SABR model (Hagan et al., 2002) designed to accurately depict the shape and dynamics of the implied volatility surface (FINCAD, n.d.).

While some of the above models were primarily designed to model the volatility surface for stock options, an equally important strand of models has been developed to model swaption volatility where the underlying we seek to model is ultimately the interest rate. The problem of modelling swaption volatility is arguably more complex than for the equivalent for stock options due to the increased dimensionality of the problem. When modelling swaptions, in addition to the maturity of the option and it's strike price or rate, the tenor of the underlying swap must also be taken into consideration. This leads to what has been called a 'volatility cube' rather than the more recogniseable volatility surface.

This short report seeks to provide a comparison of the more prominent and recent models introduced in this area of research alongside numerical implementation of a number of selected models to the US swaption market. The reader is encouraged to view and interact with the results of the various implementations as they move through the report. These can be found at https://01389888.github.io/AP/ in the section relevant to the reader.

Data

The data used throughout this report is swaption data from Bloomberg collected on 09/07/2018. Swaption maturities of 3m, 6m, 1y, 2y, 3y, 4y, 5y, 10y, 15y and 30y were used with underlying swap tenors of 1y, 2y, 3y, 4y, 5y, 10y, 15y, 20y and 30y for each maturity. This data was collected for swaptions that were ATM as well as for those with strikes of -200bps, -150bps, -100bps, -50bps, +50bps, +100bps, +150bps and +200bps relative to the ATM rate.

The data can be found in Appendix A.

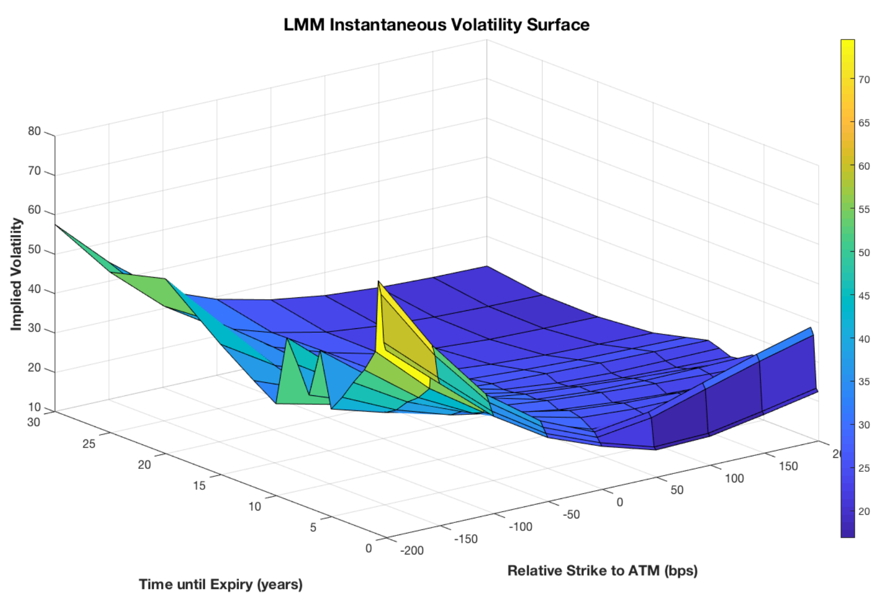

Figure 1: Market implied volatility surface for 5Y tenor

Chapter 1

Libor Market Model (LMM)

Theory

The LMM model concerns itself with the modelling of the forward rates and their instantaneous volatilities. Intuitively, these forward rates across different time horizons must be correlated to some extent and so one of the primary concerns when implementing the LMM is how to model these correlations (Qu, 2016).

To compose the standard formulation of the LMM, let $f_{i,i+1}(t)$ be the forward rate from time T_i to T_{i+1}, and let $P(t, T_i)$ represent the price of a zero coupon bond maturing at time T_i, at time t. Then under no arbitrage,

$$f_{i,i+1}(t)P(t, T_{i+1}) = \frac{P(t, T_i) - P(t, T_{i+1})}{\tau_{i,i+1}}, \tag{1.1}$$

where $\tau_{i,i+1} = T_{i+1} - T_i$. Let Q_i be the measure for the numeraire $P(t, T_{i+1})$. Then $f_{i,i+1}(t)$ must be a martingale with respect to Q_i. Under the log-normal assumption, we can now model the forward rate as:

$$df_{i,i+1} = \sigma_i(t)f_{i,i+1}(t)dW_i^{Q_i}, \tag{1.2}$$

where $\sigma_i(t)$ is the instantaneous volatility at time t.

Consideration must be made for that fact that while $f_{i,i+1}$ is a martingale under Q_i, the other forward rates $f_{j,j+1}$, are not. Using a change of measure, Qu (2016) gives the process to describe all the forwards as:

$$\frac{df_{j,j+1}}{f_{j,j+1}} = \mu_i^j(t)dt + \sigma_i(t)dW_j^{Q_i}, \tag{1.3}$$

where,

$$\mu_i^j(t) = \begin{cases} \sum_{k=i+1}^{j} \frac{\tau_{k,k+1} f_{k,k+1}(t) \sigma_k \sigma_j \rho_{jk}}{1+\tau_{k,k+1} f_{k,k+1}(t)} & i < j \\ 0 & i = j \\ -\sum_{k=i+1}^{j} \frac{\tau_{k,k+1} f_{k,k+1}(t) \sigma_k \sigma_j \rho_{jk}}{1+\tau_{k,k+1} f_{k,k+1}(t)} & i < j. \end{cases}$$

A number of key points regarding this formulation of the LMM are as follows:

- Due to the state dependency of $\mu_i^j(t)$, the process is not Markovian and thus is not able to be modelled by standard techniques such as a PDE solver or a tree (Qu, 2016).
- The model is popular because of its fluency with Black's formula for caps but due to the fact that the log-normal assumption on the Libor rate does not lead to log-normal forward rates, it is less compatible with Black's swaption formula and approximations are required (Bandera, 2008).

Given the forward rate dynamics in equation 1.3, the joint dynamics of the forwards rates can be represented as:

$$\begin{bmatrix} \frac{df_{1,2}}{f_{1,2}} \\ \vdots \\ \frac{df_{n,n+1}}{f_{n,n+1}} \end{bmatrix} = \begin{bmatrix} \mu_1 \\ \vdots \\ \mu_n \end{bmatrix} dt + \begin{bmatrix} \sigma_1 & \dots & 0 \\ \vdots & \sigma_i & \vdots \\ 0 & \dots & \sigma_n \end{bmatrix} \begin{bmatrix} dW_1 \\ \vdots \\ dW_n \end{bmatrix}, \tag{1.4}$$

and attention can be turned to the modelling of correlations between forward rates.

There are a couple of ways to model these correlations. The first is the most complex and begins by deriving the terminal correlation of forward rates as,

$$Corr(f_{i,i+1}(T), f_{j,j+1}(T)) = \frac{\mathbb{E}[(f_{i,i+1}(T) - \mathbb{E}[f_{i,i+1}(T)])(f_{j,j+1}(T) - \mathbb{E}[f_{j,j+1}(T)])]}{\sqrt{\mathbb{E}[(f_{i,i+1}(T) - \mathbb{E}[f_{i,i+1}(T)])^2]}\sqrt{\mathbb{E}[(f_{j,j+1}(T) - \mathbb{E}[f_{j,j+1}(T)])^2]}}. \tag{1.5}$$

While equation 1.5 can be simulated using Monte-Carlo, it is more often approximated as,

$$Corr(f_{i,i+1}(T), f_{j,j+1}(T)) = \frac{\exp(\int_0^T \sigma_i(t)\sigma_j(t)\rho_{i,j}dt) - 1}{\sqrt{\exp(\int_0^T \sigma_i(t)^2 dt) - 1}\sqrt{\exp(\int_0^T \sigma_j(t)^2 dt) - 1}}, \tag{1.6}$$

and then approximated further by taking the first order expansion of the exponentials:

$$Corr(f_{i,i+1}(T), f_{j,j+1}(T)) = \rho_{i,j} \frac{\int_0^T \sigma_i(t)\sigma_j(t)\rho_{i,j}dt}{\sqrt{\int_0^T \sigma_i(t)^2 dt}\sqrt{\int_0^T \sigma_j(t)^2 dt}}. \tag{1.7}$$

To calculate the desired instantaneous forward rate correlations from here requires parameterisation of the instantaneous volatilities and correlations which is possible but "very arduous" (Rebonato, 2002, pp175).

The second approach to modelling the instantaneous correlations is to give them an explicit functional form. Some sensible suggestions provided by Qu (2016) are shown in table 1.1. The parameters are arbitrarily chosen as $\beta = 0.5$ and $\rho = 30\%$ and $\Delta T = |T_i - T_j|$ and used to plot the curves shown in figure 1.1 (Qu, 2016). The intuition behind the use of these decaying functions is fairly obvious as when $\Delta T = 0$ (i.e. $i = j$), it is clear that the correlation should be 1 and it is reasonable to expect a decrease in correlation from there with increasingly different forward rate maturities.

Functional Form	**Formula**
Exponential	$\rho(\Delta T) = \tilde{\rho} + (1 - \tilde{\rho})\exp(-\beta \Delta T)$
Tanh	$\rho(\Delta T) = \tilde{\rho} + (1 - \tilde{\rho})(1 - \tanh(\beta \Delta T))$
Cosh	$\rho(\Delta T) = \tilde{\rho} + \frac{(1-\tilde{\rho})}{\cosh(\beta \Delta T)}$

Table 1.1: Instantaneous correlation functions

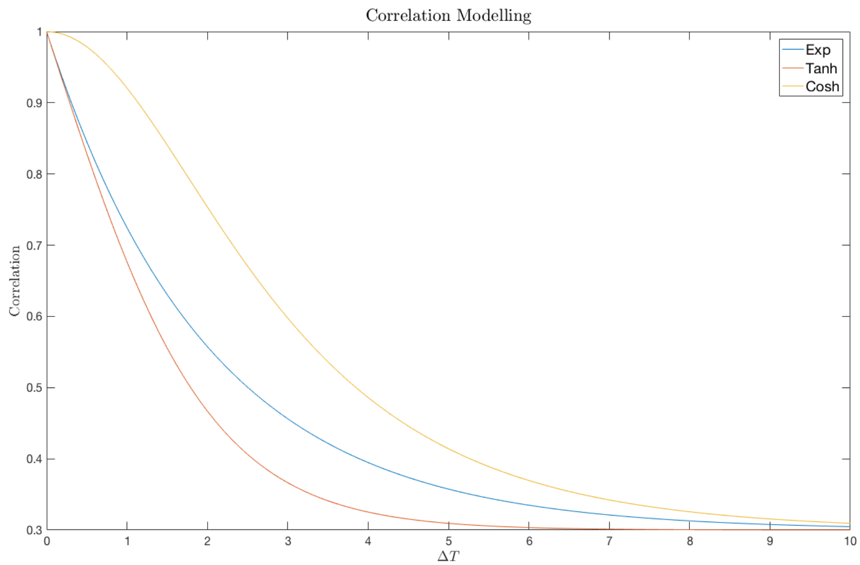

Figure 1.1: Instantaneous correlation functions

Calibration

The swaption Black volatility is given by (Rebonato, 2002),

$$[\sigma_{Black}^{(\alpha\times\beta)}]^2 = \frac{1}{T_\alpha}\int_0^{T_\alpha} \sigma^2_{(\alpha\times\beta)}(u)dt, \tag{1.8}$$

where,

$$\sigma^2_{(\alpha\times\beta)}(t) = \sum_{i,j=\alpha}^{\beta-1} \frac{w_i(t)w_j(t)f_{i,i+1}(t)f_{j,j+1}(t)\rho_{i,j}}{S_{\alpha,\beta}(t)} \int_0^{T_\alpha} \sigma_i(t)\sigma_j(t)dt, \tag{1.9}$$

is the instantaneous swaption volatility that under and approximation of the integral can be stripped from the market implied volatility using equation 1.8.

$S_{\alpha,\beta}$ denotes the forward swap rate at time t for a swap with payment dates $T_{\alpha+1}, ..., T_\beta$ and is given by,

$$S_{\alpha,\beta}(t) = \sum_{i,j=\alpha}^{\beta-1} w_i(t)f_{i,i+1}(t), \tag{1.10}$$

where,

$$w_i(t) = \frac{\tau_{i,i+1} \prod_{j=\alpha}^{i} \frac{1}{1+\tau_{j,j+1} f_{j,j+1}(t)}}{\sum_{k=\alpha+1}^{\beta} \tau_{k,k+1} \prod_{j=\alpha}^{i} \frac{1}{1+\tau_{j,j+1} f_{j,j+1}(t)}}. \tag{1.11}$$

Under the assumption of piecewise constant instantaneous volatilities, the integral in equation 1.8 can be simplified to a sum and then applying Rebonato's freezing approximation (Jackel, Rebonato, 2000) results in the following:

$$\begin{aligned} \sigma^2_{(\alpha\times\beta)}(t) &= \sum_{i,j=\alpha}^{\beta-1} \frac{w_i(t) w_j(t) f_{i,i+1}(t) f_{j,j+1}(t) \rho_{i,j}}{S_{\alpha,\beta}(t)} \sum_{h=0}^{\alpha} \tau_{h,h+1} \sigma_{i,h} \sigma_{j,h} \\ &\approx \sum_{i,j=\alpha}^{\beta-1} \frac{w_i(0) w_j(0) f_{i,i+1}(0) f_{j,j+1}(0) \rho_{i,j}}{S_{\alpha,\beta}(0)} \sum_{h=0}^{\alpha} \tau_{h,h+1} \sigma_{i,h} \sigma_{j,h}. \end{aligned} \tag{1.12}$$

Substituting the above into equation 1.8 and optimising results in a set of forward rates and instantaneous swap volatilities calibrated to the implied volatilities as given in the market. It is important to note that while the LMM is very effective at calibrating to an ATM swaption implied volatility surface, it is far less effective when calibrating to ITM or OTM surfaces and fails to accurately represent the smile (Qu, 2016).

Numerical implementation of the LMM model has been omitted from this report to allow for implementation of a number of the models more successful at achieving this. However, an example of the instantaneous swaption volatility surface stripped from market implied volatilities using equation 1.8 for the 5 year swaption tenor can be seen in figure 1.2. Full results for the LMM instantaneous swaption volatility can be found in the online appendix (https://01389888.github.io/AP/).

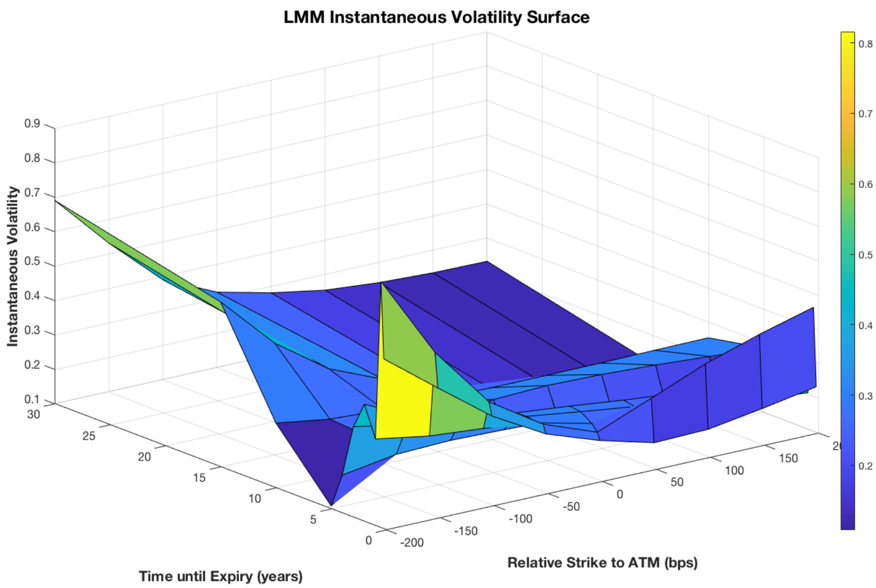

Figure 1.2: Instantaneous swaption volatility for 5Y tenor

Chapter 2

The SABR Model

Theory

The stochastic-$\alpha\beta\rho$ model - now commonly referred to as the SABR model - was developed and first published by Hagan et al. in 2002 claiming to solve an inconsistency between dynamics observed in the market and the local volatility model pioneered separately by Dupire (1994) and Derman & Kani (1994). It aims to calibrate as closely as possible to the market impiled volatility surface, accurately characterising its shape and dynamics.

Note that currently there is no generally accepted local volatility model in the fixed income setting of swaptions, although more recent work is discussed in the following chapter (Gatarek, Jablecki, 2017). That however, does not take away from the applicability of the SABR model to the swaption market.

While the introduction of the local volatility model for stock options had previously allowed for the better managing of volatility smiles and skews - an activity central to those managing books of options across a wide variety of strikes and maturities (Hagan et al., 2002) - the dynamics between the smile and the underlying is not adequately captured by the local volatility model. The discrepancy can be summed up as follows:

> "*the dynamic behavior of smiles and skews predicted by local vol models is exactly opposite the behavior observed in the marketplace: when the price of the underlying asset decreases, local vol models predict that the smile shifts to higher prices; when the price increases, these models predict that the smile shifts to lower prices. In reality, asset prices and market smiles move in the*

same direction."

- Hagan et al. (2002, pp1)

Unlike the Black model (Black, Scholes ,1973) where volatility is assumed constant and the local volatility model (Dupire, 1994, Derman & Kani, 1994) where volatility is assumed to be deterministic, the SABR model represents volatility as a random function of time. The model is then given by,

$$d\hat{F} = \hat{\alpha}\hat{F}^{\beta}dW_1, \quad \hat{F}(0) = f \tag{2.1}$$

$$d\hat{\alpha} = \nu\hat{\alpha}dW_2, \quad \hat{\alpha}(0) = \alpha, \tag{2.2}$$

$$\rho dt = dW_1 dW_2. \tag{2.3}$$

where, $\hat{F}$ is the forward rate and $\hat{\alpha}$ is the volatility.

Using an asymptotic expansion, the SABR implied volatility, σ_B is derived as:

$$\begin{aligned}\sigma_B(K,f) =& \frac{\alpha}{(fK)^{(1-\beta)/2}\left\{1 + \frac{(1-\beta)^2}{24}\log^2(\frac{f}{K}) + \frac{(1-\beta)^4}{1920}\log^4(\frac{f}{K}) + \dots\right\}} \\ &\times \left(\frac{z}{x(z)}\right) \\ &\times \left\{1 + \left[\frac{(1-\beta)^2}{24}\frac{\alpha^2}{(fK)^{(1-\beta)}} + \frac{1}{4}\frac{\rho\beta\nu\alpha}{(fK)^{(1-\beta)/2}} + \frac{2-3\rho^2}{24}\nu^2\right]t_{ex} + \dots\right\}.\end{aligned} \tag{2.4}$$

It is also worthwhile noting that the simplified formulation,

$$\sigma_{ATM} = \sigma_B(f,f) = \frac{\alpha}{f^{(1-\beta)}}\left\{1 + \left[\frac{(1-\beta)^2}{24}\frac{\alpha^2}{f^{(2-2\beta)}} + \frac{1}{4}\frac{\rho\beta\nu\alpha}{f^{(1-\beta)}} + \frac{2-3\rho^2}{24}\nu^2\right]t_{ex} + \dots\right\}, \tag{2.5}$$

can be used for at-the-money (ATM) options.

The terms left out of the asymptotic expansion and represented by '...' are small enough such that they are not required for accurate pricing (Hagan et al., 2002). Qu (2016) notes that for options with a large time to expiry, approximation errors due the asymptotic expansion do become much larger compared to a numerical solution of the associated PDE. However, it is also stated that provided these long dated options (often referred to as "the wings") do not have negative probability density, the current formulation is adequate for fitting a volatility surface (Qu, 2016). Particularly in the current low interest rate environment, a prevalent disadvantage of the SABR model is the inability to model negative interest rates. However, adaptations such as the shifted SABR model (Hagan et al, 2014) have helped remedy this problem.

One of the major advantages of the SABR model is that to price a European option, this formulation of the implied volatility can simply be used in a Black-Scholes option pricer. Alongside this, the SABR model is one of the simplest stochastic models and the nature of the solution results in computational efficiency (Hagan et al., 2002).

The role that each of the SABR parameters plays in modelling swaption volatility can be represented intuitively by individually altering parameter values from a base set and graphing a slice of the volatility surface to observe the differences. The base parameters were chosen as $\alpha = 0.03, \beta = 0.5, \rho = -0.3, \nu = 0.3$ and the value of f was arbitrarily set to 0.025.

The parameters were tested across the following values: $\alpha = \{0.01, 0.03, 0.05\}$, $\beta = \{0.3, 0.5, 0.7\}$, $\rho = \{-0.8, -0.3, 0.8\}$, $\nu = \{0.1, 0.3, 0.5\}$.

As can be seen in figure 2.1, the value of alpha determines the vertical positioning of the curve. Figure 2.2 shows how varying the β parameter changes the curvature of the curve and so β is often referred to as the "skewness" parameter (FINCAD, n.d.). Interestingly, ν also seems to govern the curvature as can be seen in figure 2.4. This has implications in the process of calibrating the parameters as will be seen in the following secion. Finally, ρ influences the rotation of the volatility smile roughly around the ATM point ($f = 0.025$) as seen in figure 2.3.

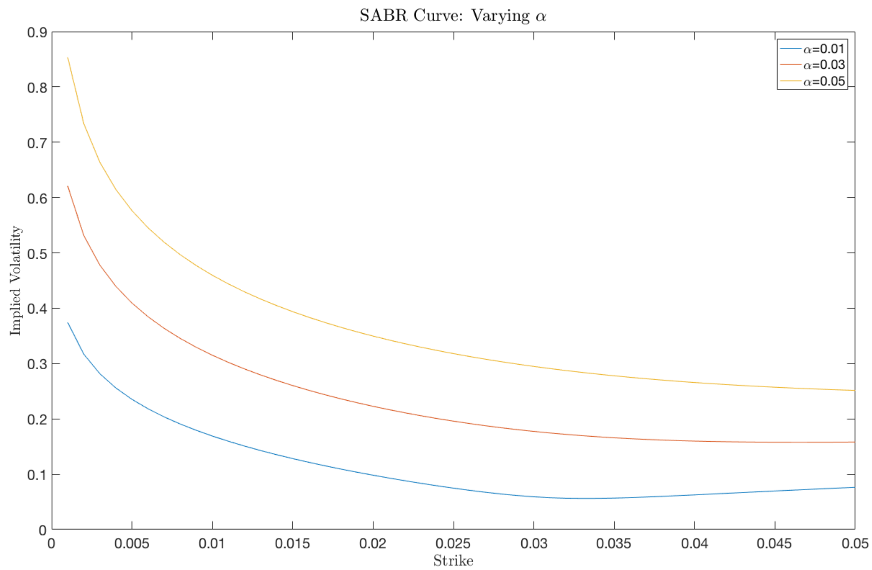

Figure 2.1: Varying α

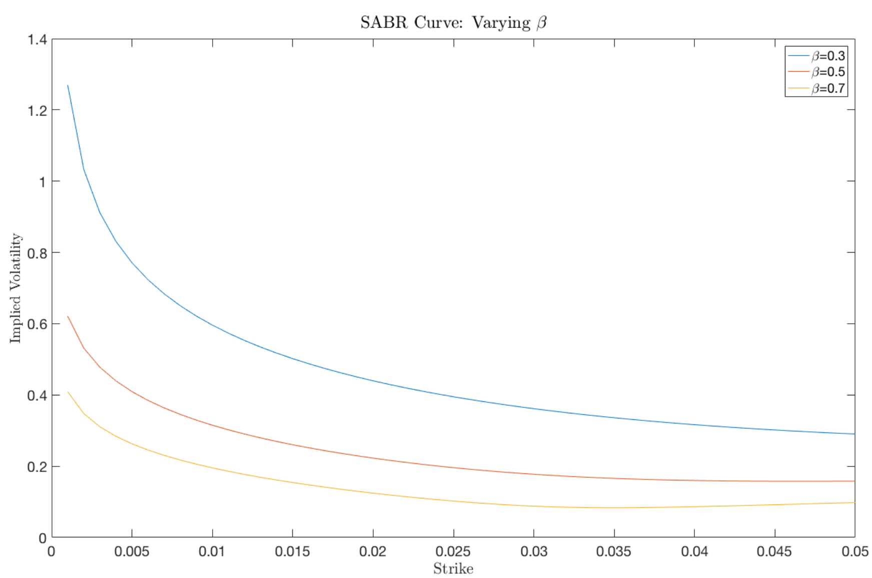

Figure 2.2: Varying β

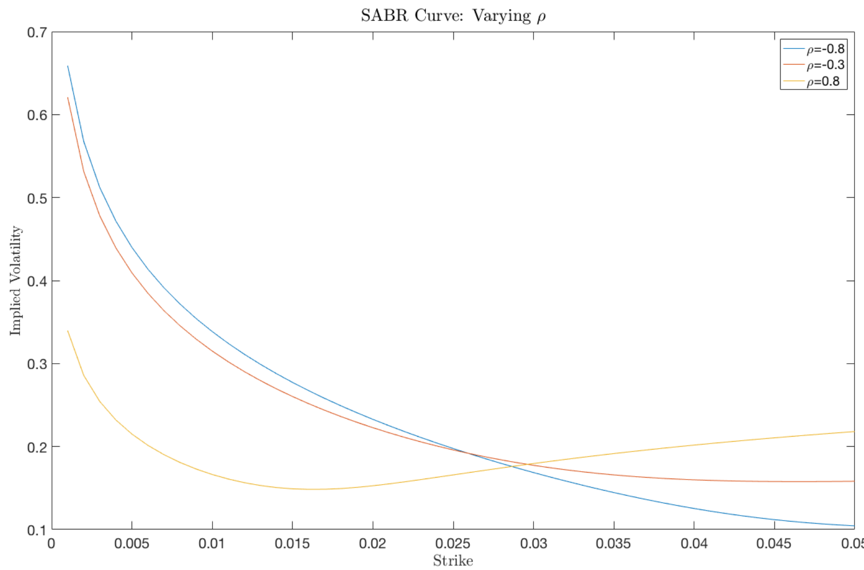

Figure 2.3: Varying ρ

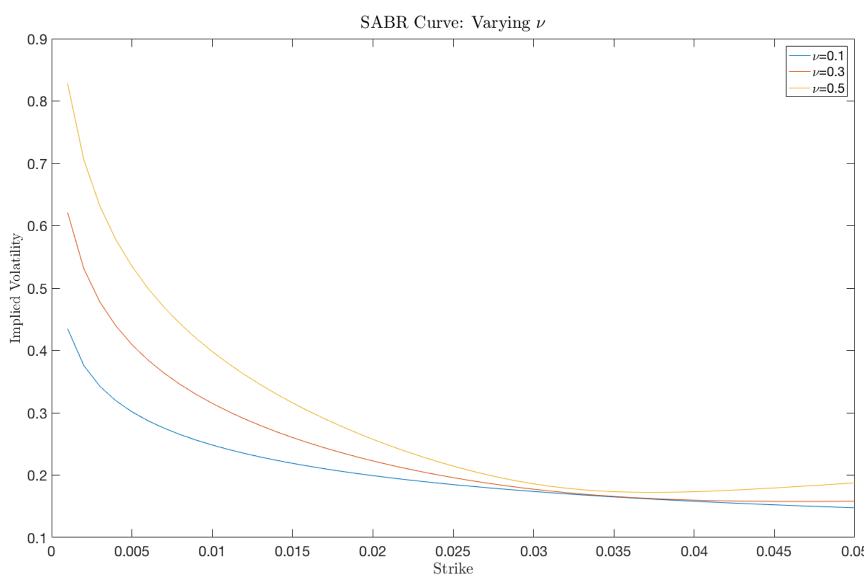

Figure 2.4: Varying ν

Calibration

There are two common approaches to calibrating the SABR parameters that are applicable to different scenarios.

The first approach is initiated by making an estimate of β that is generally about 0.5. This may seem unscientific however, due to the fact that both β and ν govern similar dynamics of the volatility smile, estimating one parameter and calibrating the other to market data has been a successful method (FINCAD, n.d.). The first approach proceeds by simultaneously calibrating all the remaining parameters by seeking to minimise,

$$\sum_i (\sigma_i - \sigma_B(\alpha, \beta, \rho, \nu; K_i, f))^2, \tag{2.6}$$

where σ_i is the market implied volatility and K_i is the corresponding strike. This approach is widely used for stock options and when calibrating caps/floors. It is less appropriate for swaptions as there is no certainty that the calibrated curve will pass through the ATM point exactly. This is demonstrated using the results from the 5Y5Y swapion as shown in figure 2.5. As the ATM point is the most liquidly traded on the curve, it is important that this is the case (FINCAD, n.d.).

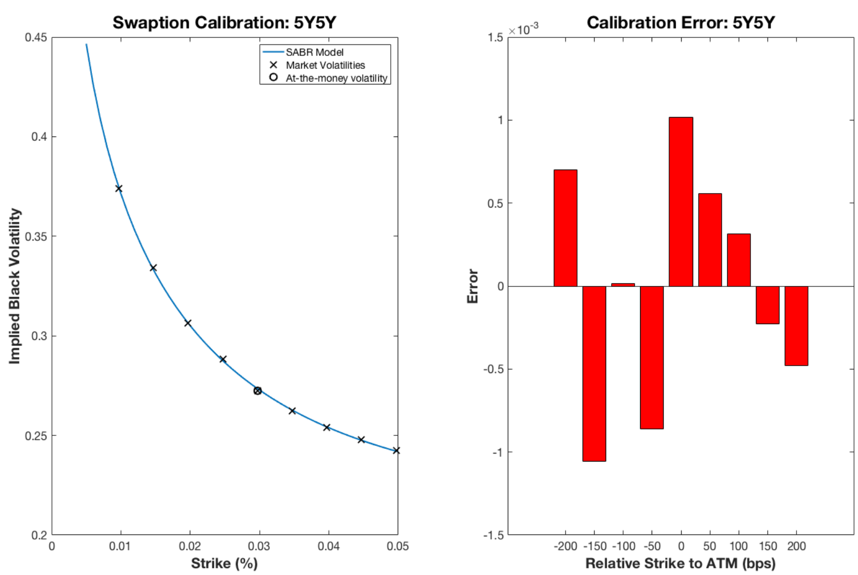

Figure 2.5: Results of 5Y5Y swaption calibration using the first method

The second, more sophisticated method of calibration solves this problem, making it the appropriate method for calibrating swaptions. As previously, β is estimated to be approximately 0.5. α is viewed as a function of ρ and ν and rearranging equation 2.5 results in the following cubic polynomial in α:

$$\alpha^3\left[\frac{(1-\beta)^2 t_{ex}}{24 f^{(2-2\beta)}}\right]+\alpha^2\left[\frac{\rho\beta\nu t_{ex}}{4 f^{(1-\beta)}}\right]+\alpha\left[1+\frac{(2-3\rho^2)\nu^2 t_{ex}}{24}\right]-\sigma_{ATM} f^{(1-\beta)}=0. \tag{2.7}$$

The smallest real root of this cubic provides the value of alpha. Thus, calibrating ρ and ν while determining α this way ensures that the calibrated curve will pass exactly through the ATM point as shown for the same 5Y5Y swaption in figure 2.6. The right hand panel of this figure makes it clear that the curve has been exactly calibrated to the ATM point as desired.

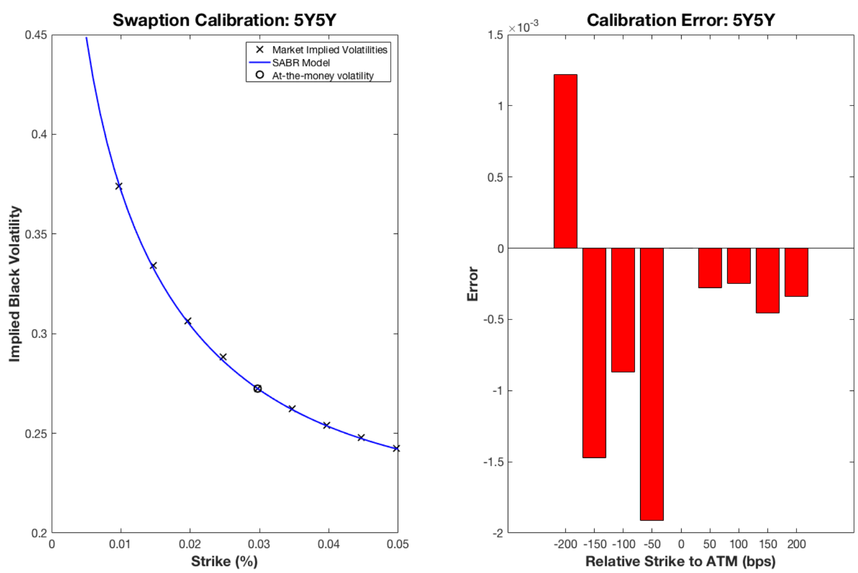

Figure 2.6: Results of 5Y5Y swaption calibration using the second method

For each swaption tenor, a calibrated volatility surface is created by simply joining the curves created through the second calibration method (Hagan et al., 2002). The fully calibrated SABR volatility surface for the 5 year tenor can be seen in figure 2.7 where the smile is easily observable along the strike axis.

Notably, Hagan et al. (2002) also point out that the calibrated parameters ρ and ν tend to be stable and do not need to be re-calibrated frequently - perhaps only every few weeks. α is less stable and may require re-calibration every few hours. The need to only re-calibrate α frequently drastically reduces the computational cost of running this model in practice.

One of the main advantages of the SABR is the ease with which the greeks can be calculated and so despite not being the main focus of this report, some details on the calculation of the swaption greeks can be found in appendix D. Full details of the calibrated SABR parameters and errors in the swaption volatility for the sophisticated method can be found in appendices B and C respectively.

Implementations of the SABR model using both the sophisticated and basic calibration methods can be found in the online appendix (https://01389888.github.io/AP/).

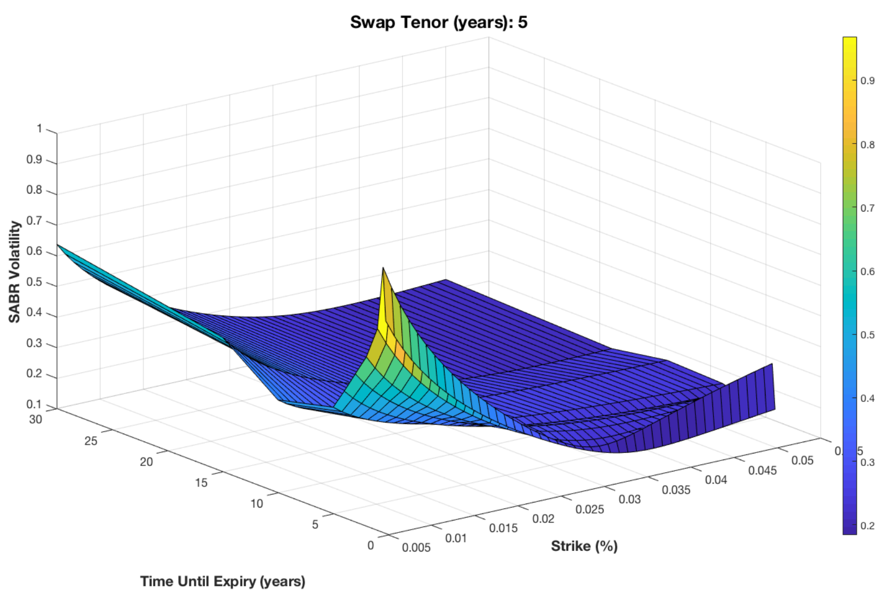

Figure 2.7: SABR swaption volatility surface for 5 year tenor

Chapter 3

Non-parametric Local Volatility Model

Theory

The non-parametric local volatility model developed for stock options by Dupire (1994), and Derman & Kani (1994) was briefly mentioned in the introduction, however until the last couple of years, an analogous non-parametric model for swaption local volatility was not available. The originally developed local volatility models are not appropriate for the fixed-income market due to their reliance on being able to calculate the derivative with respect to maturity. Qu (2016) notes that this is possible in stock option markets as the underlying has a well-defined and accepted spot process. Unfortunately this is not the case in fixed-income markets. Thus, the final model discussed is based on the paper, ‘A non-parametric local volatility for swaptions smile’ published by Gatarek and Jablecki in 2017 where such a model is introduced.

In addition to the disadvantages of local volatility models discussed at the opening of the previous chapter, Gatarek and Jablecki note their lack of success in predicting the forward volatility and forward smile dynamics (2017). Their importance however can be seen through use in the pricing of illiquid and exotic products while maintaining consistency with the corresponding vanilla products (FINCAD, n.d.). Under the Cheyette model for interest rates, “it is reasonable to assume that there is a strong link between a given swap rate and the state of the short rate, and hence that the diffusion term in the swap rate dynamics is just a deterministic function of the swap rate itself" (Gatarek, Jablecki, 2017, pp42).

The following local volatility diffusion is derived:

$$dS_T(t_{ex}) = Q_{t_{ex},T}(S_T, t)dt + \sigma_{loc}(S_T(t_{ex}), t_{ex}, T)dW^{t_{ex},T}(t_{ex}), \tag{3.1}$$

where, $S_T(t_{ex})$ is the rolling maturity swap rate given by,

$$S_T(t_{ex}) \equiv S_{t_{ex},T}(t_{ex}) = \frac{1 - P(t_{ex}, T)}{\int_{t_{ex}}^{T} P(t_{ex}, s)ds}, \tag{3.2}$$

and $P(t_{ex}, T) = \exp(-\int_{t_{ex}}^{T} f(t_{ex}, s)ds)$ is the zero coupon bond price. $Q_{t_{ex},T}(t)$ is approximated as:

$$\begin{aligned} Q_{t_{ex},T}(t) &\approx Q(t_{ex}, T) \\ &= S_{t_{ex},T}(0)\left[(S_{t_{ex},T}(0) - f(0, t_{ex})) + (f(0, T) - f(0, t_{ex}))\frac{P(0, T)}{P(0, t_{ex}) - P(0, T)}\right]. \end{aligned} \tag{3.3}$$

Given the non-linear, state dependent drift assumed in this model and under a change of measure, the below PDE is obtained:

$$\begin{aligned} \frac{\sigma_{loc}^2(K, t_{ex}, T)}{2}\frac{\partial^2 C(K, t_{ex}, T)}{\partial K^2} &= \frac{\partial C(K, t_{ex}, T)}{\partial t} + \frac{\partial C(K, t_{ex}, T)}{\partial K}q(t_{ex}, T) \\ &\quad + Q(t_{ex}, T)\frac{\partial C(K, t_{ex}, T)}{\partial K}, \end{aligned} \tag{3.4}$$

where $C(K, t_{ex}, T)$ is the undiscounted swaption payoff. It is noted by both Qu (2016) and Gatarek & Jablecki (2017) that $q(t_{ex}, T) \approx 0$ based on both empirical findings and theoretical reasoning. Thus, $q(t_{ex}, T)$ is assumed equal to 0 from this point forward.

Then,

$$\begin{aligned} &\sigma_{loc}(K, t_{ex}, T) = \\ &\sqrt{\left(\frac{\partial C(K, t_{ex}, T)}{\partial t} + Q(t_{ex}, T)\right)\left(\frac{\partial C(K, t_{ex}, T)}{\partial K}\right)\left(\frac{1}{2}\frac{\partial^2 C(K, t_{ex}, T)}{\partial K^2}\right)^{-1}}. \end{aligned} \tag{3.5}$$

Differentiation of the standard Black swaption formula enables equation 3.5 to be re-written as:

$$\sigma_{loc}(K,t,T) = \sqrt{\frac{2\frac{\partial\sigma_I}{\partial t} + \frac{\sigma_I}{t} + 2KQ(t_{ex},T)\frac{\partial\sigma_I}{\partial K}}{\frac{1}{\sigma_I t}\left(1 + \frac{Ky}{\sigma_I}\frac{\partial\sigma_I}{\partial K}\right)^2 + K^2\frac{\partial^2\sigma_I}{\partial K^2} - \frac{K^2\sigma_I t}{4}\left(\frac{\partial\sigma_I}{\partial K}\right)^2 + K\frac{\partial\sigma_I}{\partial K}}}, \quad (3.6)$$

where σ_I is the Black (log-normal) volatility implied by the market and $y = \ln(\frac{F(t_{ex},T)}{K})$. $F(t_{ex},T)$ is the rolling forward swap rate and should not be confused with the market forward swap rate. It is expressed here as,

$$F(t_{ex},T) = S_{t_{ex},T}(0)\exp\left(\int_0^{t_{ex}} Q(s,T)ds\right). \quad (3.7)$$

Using equation 3.6, the local volatility can then be calculated in a non-parametric way.

Calibration

Given the non-parametric nature of this model, its implementation relies largely on the quality of the market data. Gatarek & Jablecki highlight that although numerically efficient, the model is prone to “sinkholes”. When the term under the square root in equation 3.6 is negative, it is set to zero causing local volatilities to drop considerably in some areas of the surface. Unfortunately, this was a prominent issue throughout implementation and could be due to the interpolation techniques, numerical methods or the market data itself (Gatarek, Jablecki, 2017). Resolving these problems is likely to be the focus of study moving forward.

Spline interpolation was used to create an adequately dense set of points from which the relevant derivatives could be approximated. The methods used in the approximations are detailed in Appendix F.

As in previous chapters, the 5 year tenor is used as an illustrative example. Phase one of the process merely involves gathering the sufficient data. The market implied volatility surface for the 5 year tenor can be seen in figure 3.1.

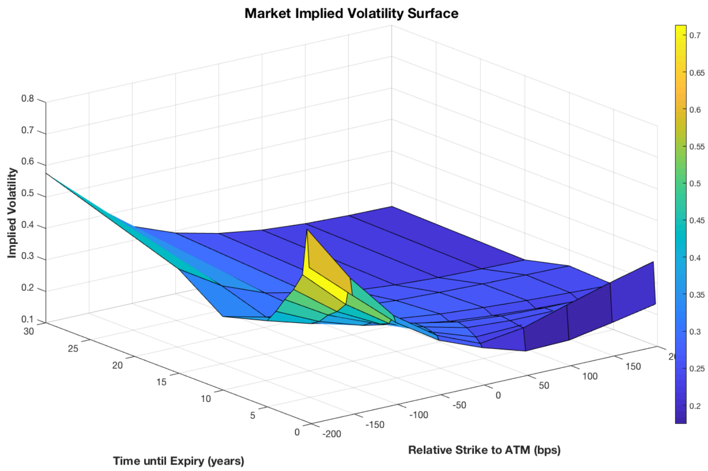

Figure 3.1: Market implied volatility surface for 5Y tenor

The market implied volatility surface is then interpolated as seen in figure 3.2 in order to enable to approximation of derivatives.

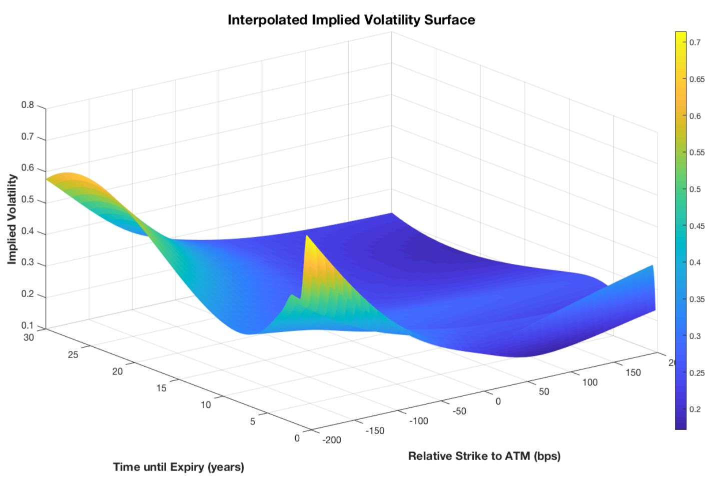

Figure 3.2: Interpolated implied volatility surface for 5Y tenor

Using equation 3.6, the local volatility surface can then be calculated and is displayed in figure 3.3.

An example of the aforementioned "sinkholes" can be seen for the lower strikes and longer maturity swaptions here. Interestingly, the areas of highest local volatility are seen for higher strike prices and shorter maturities. This is likely due to the prospect of continuing interest rate hikes by the US Federal Reserve in the short term (CNBC, 2018).

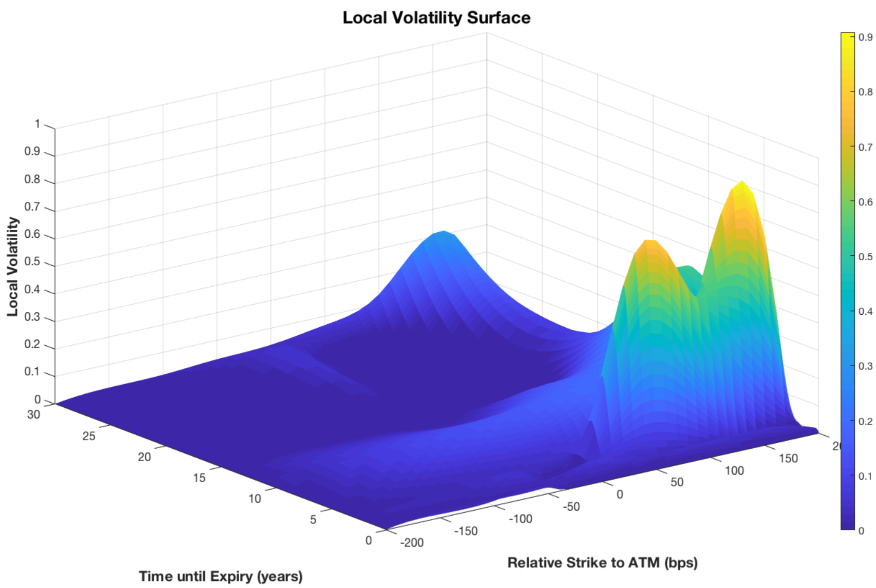

Figure 3.3: Non-parametric local volatility for 5Y tenor

The local volatility surfaces for all tenors can be found in the online appendix (https://01389888.github.io/AP/).

Conclusion

The advantages and drawbacks of 3 models used to calibrate swaption volatility surfaces and in turn, the swaption volatility cube have been discussed.

The LMM model, primarily used for the calibration of the forward curve to swaption prices results in a set of instantaneous volatilities. The most prominent drawback here is the inability to recreate the volatility smile displayed in market data. A key issue in the implementation of the LMM is the modelling of forward rate correlations. Correlations can be implied through the derivation of the terminal correlations or through explicit and sensible functional forms as suggested in chapter 1. There is also scope to model these parametrically although this has implications for computational efficiency and is not included.

The SABR model represents the forward rate as a stochastic process, is main focus of the report, and is frequently used in industry. The role of each of the SABR parameters was discussed briefly and such a parameterisation enables close calibration to market data. While two calibration methods were discussed, the second, more sophisticated method is preferred due to the importance of exact calibration to the ATM point. Despite being a parametric method, the SABR model achieves good computational efficiency due to the stability of a number of its parameters. Although it is not ideal for low interest rate environments, adaptations have been developed to remedy this. Aside from close calibration to market data, another prominent advantage of the model is the ease with which relevant greeks can be calculated - a key feature when managing large books of swaptions.

The non-parametric local volatility model for swaptions developed by Gatarek & Jablecki (2017) is at the forefront of research in this area and suggests a model equivalent to that suggested by Dupire, Derman & Kani (1994), using local volatility. Being non-parametric, computational efficiency is achieved with ease. While local volatility models display poor performance in predicting forward volatility and smile dynamics, their use is instrumental in the pricing of more exotic derivatives. The success of the model presented in this report was varying as the implementation method led to 'sinkholes' in the surface. However, this area of research is ongoing and is likely a focal point for the modelling of the swaption volatility cube moving forward.

As surfaces are a difficult aspect to depict through this medium, an interactive online appendix has been developed alongside this report to aid the intuition of the reader. It can be found at: https://01389888.github.io/AP/.

Bibliography

[1] Bandera, N., (2008) Calibration of Libor Market Model to Caps and Swaptions Market Volatilities, Available at SSRN: https://ssrn.com/abstract=1259814 [Accessed 10/07/18]

[2] Black, F., Scholes, M. (1973) The Pricing of Options and Corporate Liabilities, *The Journal of Political Ecconomy*. 81 (3), 637-654

[3] Derman, E., Kani, I. (1994) Riding on a Smile, *Risk*. 7(2), 32-39

[4] Dupire, B. (1994) Pricing with a Smile, *Risk*. 7(1), 18-20

[5] Gatarek, D., Jablecki J. (2017) A nonparametric local volatility model for swaptions smile, *Journal of Computational Finance*, 21(5), 35-52

[6] Gatarek, D., Jablecki, J., & Qu, D. (2016). Non-parametric local volatility formula for interest rate swaptions. *Risk*. 29. 120-124.

[7] Hagan, P., Kumar, D., Lesniewski, A., Woodward, D. (2002) Managing Smile Risk, *Wilmott Magazine*. 1, 84-108

[8] Hagan, P., Kumar, D., Lesniewski, A., Woodward, D. (2014) Arbitrage-Free SABR, *Wilmott Magazine*. (69), 60-75

[9] Jackel, P., Rebonato, R. (2000) Linking Caplet and Swaption Volatilities in a BGM / J Framework: Approximate Solutions, The Royal Bank of Scotland working paper

[10] Lax, P.D., Terrell, M.S., (2013) Calculus with Applications, *Springer*

[11] Merton, R. (1976) Option pricing when underlying stock returns are discontinuous, *Journal of Financial Economics*. 3, 125-144

[12] Qu, D. (2016) Manufacturing and Managing Customer-Driven Derivatives, *Wiley*

[13] Rebonato, R. (2002) Modern Pricing of Interest Rate Derivatives: The LIBOR Market and Beyond, *Princeton University Press*

[14] Travaglini, G. (2016) SABR Calibration in Python, Available at SSRN: https://ssrn.com/abstract=2725485 [Accessed 12/07/2018]

[15] CNBC (2018) Fed hike and economic forecast seen as a double-edged sword for markets, Available at: https://www.cnbc.com/2018/03/21/fed-hike-and-forecast-seen-as-a-double-edged-sword-for-markets.html [Accessed: 22/07/2018]

[16] FINCAD (n.d.) *Manage Smile Risk with the SABR Model of Stochastic Volatility*, Available from: http://www.fincad.com/resources/resource-library/article/manage-smile-risk-sabr-model-stochastic-volatility [Accessed 15/07/2018]

Appendix A

Data

ATM	Tenor								
Expiry	1Yr	2Yr	3Yr	4Yr	5Yr	10Yr	15Yr	20Yr	30Yr
3Mo	14.49	17.95	20.02	20.41	21.62	20.66	21.99	22.01	22.2
6Mo	15.22	19.31	20.75	22.46	22.71	23.05	22.91	22.93	23.56
1Yr	18.63	21.82	23.19	23.96	24.24	23.26	23.01	22.89	24.76
2Yr	22.06	24.75	25.27	25.74	26.12	25.41	23.93	25.05	25.86
3Yr	25.77	26.14	26.47	26.69	26.85	26.17	24.13	23.67	26.45
4Yr	27.64	27.65	27.53	27.34	25.98	26.53	24.2	24.1	26.41
5Yr	28.78	28.39	28	26.61	27.25	26.61	26	25.43	26.43
10Yr	27.23	26.04	24.56	26.6	26.19	25.65	24.49	24.1	24.89
15Yr	26.28	25.57	25.03	23.45	23.89	24	23.16	22.6	23.16
30Yr	28.24	27.01	26.89	26.5	26.13	23.72	24.63	24.38	24.54

Table A.1: ATM Implied Volatility

Forwards	Tenor								
Expiry	1Yr	2Yr	3Yr	4Yr	5Yr	10Yr	15Yr	20Yr	30Yr
3MO	2.7758	2.8862	2.9209	2.9258	2.9232	2.9476	2.9677	2.9612	2.9242
6MO	2.8853	2.9396	2.9538	2.9489	2.9416	2.9608	2.9759	2.967	2.9276
1YR	2.9962	2.9976	2.9814	2.9652	2.9555	2.9744	2.9832	2.9713	2.9292
2YR	2.9988	2.9734	2.954	2.9444	2.9428	2.9774	2.9803	2.966	2.9211
3YR	2.9473	2.9306	2.9252	2.9278	2.9355	2.9777	2.9769	2.9595	2.9123
4YR	2.9134	2.9136	2.9208	2.9323	2.9455	2.9842	2.9764	2.9554	2.9055
5YR	2.9139	2.9247	2.939	2.9542	2.9689	2.9936	2.978	2.9527	2.8995
10YR	3.051	3.0444	3.0331	3.0281	3.0223	2.9836	2.9455	2.9103	2.8445
15YR	2.964	2.9578	2.9539	2.9463	2.9388	2.8978	2.8608	2.8276	2.7599
30YR	2.7364	2.7257	2.715	2.7059	2.695	2.6429	2.6081	2.5683	2.2582

Table A.2: ATM Swap Forward Rates

-50bps	Tenor								
Expiry	1Yr	2Yr	3Yr	4Yr	5Yr	10Yr	15Yr	20Yr	30Yr
3Mo	18.45	22.54	25.04	25.53	27.04	25.78	27.38	27.41	27.77
6Mo	19.1	24.11	25.87	28.01	28.34	28.73	28.51	28.56	29.44
1 Yr	22.12	25.91	27.55	28.5	28.85	27.66	27.34	27.22	29.52
2 Yr	24.81	27.86	28.47	29.01	29.44	28.61	26.93	28.21	29.18
3 Yr	28.37	28.79	29.16	29.4	29.56	28.78	26.54	26.05	29.15
4 Yr	30.04	30.05	29.91	29.7	28.21	28.78	26.26	26.17	28.71
5 Yr	30.49	30.08	29.65	28.17	28.84	28.15	27.52	26.93	28.02
10 Yr	28.27	27.03	25.5	27.62	27.19	26.65	25.45	25.07	25.9
15 Yr	29.08	28.3	27.7	25.95	26.46	26.61	25.71	25.13	25.81
30 Yr	31.63	30.27	30.14	29.72	29.32	26.67	27.74	27.5	28.12

Table A.3: -50bps Implied Volatility

+50bps	Tenor								
Expiry	1Yr	2Yr	3Yr	4Yr	5Yr	10Yr	15Yr	20Yr	30Yr
3Mo	11.69	14.5	16.18	16.5	17.47	16.71	17.78	17.79	17.94
6Mo	16.54	20.93	22.46	24.32	24.6	24.95	24.78	24.81	25.54
1Yr	18.98	22.23	23.62	24.42	24.71	23.7	23.44	23.33	25.24
2Yr	21.37	23.96	24.46	24.92	25.28	24.61	23.17	24.25	25.03
3Yr	24.67	25.02	25.33	25.54	25.69	25.06	23.11	22.67	25.31
4Yr	26.3	26.31	26.2	26.02	24.73	25.27	23.06	22.95	25.12
5Yr	27.67	27.31	26.94	25.6	26.22	25.62	25.03	24.47	25.42
10Yr	26.7	25.53	24.08	26.08	25.67	25.14	24	23.61	24.37
15Yr	24.99	24.31	23.79	22.29	22.71	22.8	21.98	21.44	21.95
30Yr	26.09	24.95	24.83	24.47	24.12	21.88	22.7	22.44	22.43

Table A.4: +50bps Implied Volatility

-100bps	Tenor								
Expiry	1Yr	2Yr	3Yr	4Yr	5Yr	10Yr	15Yr	20Yr	30Yr
3 Mo	24.66	29.88	33.13	33.76	35.77	34.06	36.12	36.18	36.73
6 Mo	25.66	32.1	34.36	37.24	37.72	38.11	37.74	37.86	39.27
1 Yr	26.44	30.97	33	34.19	34.64	33.14	32.73	32.64	35.55
2 Yr	28.02	31.54	32.28	32.92	33.42	32.37	30.47	31.95	33.19
3 Yr	31.4	31.9	32.32	32.58	32.74	31.78	29.31	28.81	32.34
4 Yr	32.87	32.88	32.71	32.46	30.81	31.36	28.63	28.56	31.43
5 Yr	32.45	32	31.53	29.94	30.64	29.87	29.22	28.62	29.84
10 Yr	29.36	28.08	26.49	28.7	28.26	27.72	26.51	26.14	27.07
15 Yr	32.22	31.37	30.72	28.8	29.38	29.65	28.73	28.15	29.1
30 Yr	37.12	35.56	35.44	34.98	34.54	31.58	32.97	32.83	34.96

Table A.5: -100bps Implied Volatility

+100bps	Tenor								
Expiry	1Yr	2Yr	3Yr	4Yr	5Yr	10Yr	15Yr	20Yr	30Yr
3Mo	12.15	14.87	16.53	16.85	17.85	17.02	18.08	18.11	18.33
6Mo	19.4	24.46	26.24	28.42	28.76	29.14	28.92	28.97	29.88
1Yr	20.08	23.52	25.01	25.86	26.17	25.1	24.81	24.7	26.76
2Yr	21.32	23.92	24.43	24.88	25.25	24.57	23.13	24.21	25.01
3Yr	24.15	24.5	24.81	25.01	25.16	24.54	22.62	22.19	24.78
4Yr	25.39	25.4	25.29	25.12	23.88	24.4	22.26	22.16	24.25
5Yr	26.79	26.44	26.08	24.79	25.4	24.81	24.24	23.7	24.6
10Yr	26.3	25.15	23.71	25.69	25.29	24.76	23.63	23.25	24
15Yr	24.17	23.51	23.01	21.55	21.96	22.04	21.25	20.73	21.21
30Yr	24.96	23.87	23.75	23.41	23.07	20.92	21.71	21.46	21.44

Table A.6: +100bps Implied Volatility

-150bps	Tenor								
Expiry	1Yr	2Yr	3Yr	4Yr	5Yr	10Yr	15Yr	20Yr	30Yr
3Mo	33.11	39.76	43.95	44.76	47.44	45.06	47.71	47.83	48.71
6Mo	36.09	44.84	47.92	51.96	52.67	53.11	52.5	52.72	54.95
1Yr	33.25	38.94	41.58	43.16	43.79	41.8	41.24	41.18	45.09
2Yr	33.67	38.02	39	39.82	40.43	39	36.69	38.55	40.27
3Yr	36.64	37.29	37.8	38.1	38.25	36.96	34.09	33.57	37.89
4Yr	37.62	37.63	37.43	37.09	35.16	35.66	32.58	32.57	36.01
5Yr	35.52	35.02	34.46	32.69	33.42	32.54	31.86	31.26	32.7
10Yr	31.3	29.95	28.26	30.62	30.15	29.64	28.41	28.08	29.21
15Yr	37.97	37	36.24	34.02	34.74	35.24	34.34	33.79	35.27
30Yr	47.94	46.01	45.94	45.41	44.93	41.47	43.61	43.76	49.22

Table A.7: -150bps Implied Volatility

+150bps	Tenor								
Expiry	1Yr	2Yr	3Yr	4Yr	5Yr	10Yr	15Yr	20Yr	30Yr
3Mo	13.96	17	18.87	19.23	20.37	19.41	20.6	20.63	20.92
6Mo	22.12	27.88	29.91	32.39	32.77	33.2	32.94	33.01	34.06
1Yr	21.36	25.01	26.6	27.52	27.86	26.7	26.4	26.28	28.5
2Yr	21.76	24.43	24.95	25.42	25.8	25.08	23.61	24.73	25.56
3Yr	24.1	24.44	24.75	24.96	25.1	24.47	22.56	22.14	24.74
4Yr	24.87	24.88	24.77	24.61	23.39	23.9	21.8	21.7	23.76
5Yr	26.14	25.8	25.45	24.19	24.78	24.21	23.65	23.12	24
10Yr	26.09	24.94	23.52	25.48	25.08	24.56	23.44	23.06	23.8
15Yr	23.82	23.18	22.68	21.25	21.66	21.74	20.97	20.46	20.95
30Yr	24.41	23.35	23.24	22.9	22.58	20.49	21.26	21.03	21.1

Table A.8: +150bps Implied Volatility

-200bps	Tenor								
Expiry	1Yr	2Yr	3Yr	4Yr	5Yr	10Yr	15Yr	20Yr	30Yr
3Mo	41.55	49.81	55.02	56.03	59.39	56.39	59.68	59.83	60.98
6Mo	48.87	60.74	64.93	70.4	71.36	71.96	71.14	71.44	74.43
1Yr	42.71	50.02	53.42	55.46	56.27	53.71	52.98	52.91	57.96
2Yr	42.04	47.5	48.74	49.77	50.54	48.72	45.84	48.17	50.35
3Yr	44.33	45.13	45.75	46.11	46.29	44.69	41.22	40.61	45.88
4Yr	44.38	44.4	44.15	43.74	41.45	42	38.39	38.38	42.5
5Yr	39.79	39.22	38.58	36.59	37.39	36.39	35.64	34.99	36.65
10Yr	34.6	33.12	31.27	33.89	33.39	32.88	31.54	31.2	32.5
15Yr	47.13	45.94	45	42.25	43.15	43.8	42.71	42.06	43.94
30Yr	61.44	58.97	58.89	58.22	57.61	53.2	55.98	56.2	63.46

Table A.9: -200bps Implied Volatility

+200bps	Tenor								
Expiry	1Yr	2Yr	3Yr	4Yr	5Yr	10Yr	15Yr	20Yr	30Yr
3Mo	15.93	19.35	21.46	21.86	23.17	22.06	23.39	23.44	23.79
6Mo	24.6	30.97	33.21	35.97	36.4	36.86	36.57	36.64	37.84
1Yr	22.64	26.51	28.21	29.18	29.55	28.31	27.98	27.87	30.24
2Yr	22.31	25.05	25.59	26.08	26.46	25.72	24.22	25.36	26.23
3Yr	24.16	24.51	24.82	25.03	25.17	24.54	22.62	22.2	24.81
4Yr	24.49	24.49	24.39	24.23	23.03	23.54	21.47	21.37	23.39
5Yr	25.58	25.24	24.9	23.68	24.26	23.71	23.16	22.63	23.48
10Yr	25.89	24.75	23.34	25.28	24.89	24.37	23.26	22.89	23.62
15Yr	23.58	22.94	22.45	21.03	21.43	21.52	20.75	20.24	20.73
30Yr	24.2	23.15	23.04	22.7	22.38	20.31	21.07	20.84	20.88

Table A.10: +200bps Implied Volatility

Appendix B

SABR Parameters

Tenor	Expiry	α	β	ρ	ν	Tenor	Expiry	α	β	ρ	ν
1Y	3Mo	0.0241	0.5000	-0.4997	0.5980	5Y	3Mo	0.0367	0.5000	-0.5158	0.9023
	6Mo	0.0249	0.5000	-0.0695	0.9683		6Mo	0.0361	0.5000	-0.0698	1.3900
	1Yr	0.0310	0.5000	-0.0941	0.6952		1Yr	0.0392	0.5000	-0.0946	0.8826
	2Yr	0.0368	0.5000	-0.1473	0.5103		2Yr	0.0426	0.5000	-0.1486	0.5944
	3Yr	0.0426	0.5000	-0.1574	0.4231		3Yr	0.0442	0.5000	-0.1574	0.4382
	4Yr	0.0459	0.5000	-0.1969	0.3287		4Yr	0.0435	0.5000	-0.1965	0.3117
	5Yr	0.0484	0.5000	-0.0360	0.1704		5Yr	0.0463	0.5000	-0.0373	0.1665
	10Yr	0.0452	0.5000	0.2817	0.1968		10Yr	0.0434	0.5000	0.2834	0.1884
	15Yr	0.0394	0.5000	-0.2540	0.4037		15Yr	0.0363	0.5000	-0.2542	0.3736
	30Yr	0.0360	0.5000	-0.4198	0.4952		30Yr	0.0340	0.5000	-0.4206	0.4664
2Y	3Mo	0.0303	0.5000	-0.5119	0.7476	10Y	3Mo	0.0352	0.5000	-0.5180	0.8652
	6Mo	0.0313	0.5000	-0.0698	1.2046		6Mo	0.0367	0.5000	-0.0700	1.4094
	1Yr	0.0359	0.5000	-0.0947	0.8045		1Yr	0.0379	0.5000	-0.0950	0.8517
	2Yr	0.0407	0.5000	-0.1482	0.5670		2Yr	0.0417	0.5000	-0.1479	0.5813
	3Yr	0.0430	0.5000	-0.1573	0.4277		3Yr	0.0434	0.5000	-0.1564	0.4302
	4Yr	0.0459	0.5000	-0.1972	0.3288		4Yr	0.0446	0.5000	-0.1957	0.3198
	5Yr	0.0478	0.5000	-0.0370	0.1706		5Yr	0.0454	0.5000	-0.0373	0.1645
	10Yr	0.0433	0.5000	0.2797	0.1886		10Yr	0.0423	0.5000	0.2842	0.1839
	15Yr	0.0385	0.5000	-0.2541	0.3949		15Yr	0.0363	0.5000	-0.2561	0.3740
	30Yr	0.0349	0.5000	-0.4194	0.4788		30Yr	0.0316	0.5000	-0.4209	0.4311
3Y	3Mo	0.0340	0.5000	-0.5154	0.8358	15Y	3Mo	0.0376	0.5000	-0.5202	0.9213
	6Mo	0.0334	0.5000	-0.0699	1.2844		6Mo	0.0366	0.5000	-0.0699	1.4023
	1Yr	0.0379	0.5000	-0.0949	0.8493		1Yr	0.0376	0.5000	-0.0950	0.8435
	2Yr	0.0414	0.5000	-0.1483	0.5769		2Yr	0.0395	0.5000	-0.1479	0.5498
	3Yr	0.0435	0.5000	-0.1573	0.4323		3Yr	0.0402	0.5000	-0.1569	0.3988
	4Yr	0.0458	0.5000	-0.1973	0.3281		4Yr	0.0408	0.5000	-0.1955	0.2932
	5Yr	0.0473	0.5000	-0.0368	0.1684		5Yr	0.0443	0.5000	-0.0373	0.1607
	10Yr	0.0410	0.5000	0.2791	0.1781		10Yr	0.0403	0.5000	0.2855	0.1745
	15Yr	0.0379	0.5000	-0.2543	0.3876		15Yr	0.0350	0.5000	-0.2580	0.3625
	30Yr	0.0348	0.5000	-0.4199	0.4768		30Yr	0.0323	0.5000	-0.4244	0.4444
4Y	3Mo	0.0347	0.5000	-0.5160	0.8528	20Y	3Mo	0.0376	0.5000	-0.5194	0.9213
	6Mo	0.0358	0.5000	-0.0698	1.3771		6Mo	0.0366	0.5000	-0.0701	1.4034
	1Yr	0.0389	0.5000	-0.0948	0.8739		1Yr	0.0374	0.5000	-0.0951	0.8395
	2Yr	0.0420	0.5000	-0.1483	0.5863		2Yr	0.0411	0.5000	-0.1483	0.5730
	3Yr	0.0439	0.5000	-0.1573	0.4360		3Yr	0.0394	0.5000	-0.1566	0.3916
	4Yr	0.0455	0.5000	-0.1969	0.3266		4Yr	0.0405	0.5000	-0.1962	0.2908
	5Yr	0.0451	0.5000	-0.0375	0.1618		5Yr	0.0432	0.5000	-0.0385	0.1555
	10Yr	0.0441	0.5000	0.2831	0.1915		10Yr	0.0395	0.5000	0.2860	0.1710
	15Yr	0.0359	0.5000	-0.2540	0.3673		15Yr	0.0342	0.5000	-0.2589	0.3543
	30Yr	0.0344	0.5000	-0.4202	0.4716		30Yr	0.0319	0.5000	-0.4270	0.4397

Table B.1: SABR Parameters

Tenor	Expiry	α	β	ρ	ν
30Y	3Mo	0.0377	0.5000	-0.5160	0.9268
	6Mo	0.0372	0.5000	-0.0699	1.4354
	1Yr	0.0398	0.5000	-0.0951	0.8983
	2Yr	0.0420	0.5000	-0.1487	0.5888
	3Yr	0.0434	0.5000	-0.1574	0.4321
	4Yr	0.0439	0.5000	-0.1978	0.3148
	5Yr	0.0444	0.5000	-0.0383	0.1573
	10Yr	0.0403	0.5000	0.2951	0.1719
	15Yr	0.0345	0.5000	-0.2620	0.3598
	30Yr	0.0323	0.5000	-0.4768	0.4181

Table B.2: SABR Parameters

Appendix C

SABR Calibration Errors

Tenor 1Y($\times 10^2$)	Moneyness								
Expiry	-200bps	-150bps	-100bps	-50bps	ATM	50bps	100bps	150bps	200bps
3Mo	10.43	-12.34	-2.01	3.10	0.00	8.11	6.72	-0.63	-8.73
6Mo	-1.81	-3.51	7.76	1.95	0.00	-0.35	0.51	1.01	0.49
1Yr	2.03	-0.47	-1.42	-7.80	0.00	-4.79	-3.23	-0.32	2.24
2Yr	-1.17	1.20	1.99	-4.38	0.00	-2.27	-1.25	-0.28	1.47
3Yr	0.38	-0.42	0.72	-3.78	0.00	-1.19	-0.90	-0.76	0.84
4Yr	0.99	-1.57	0.46	-2.50	0.00	-0.88	-0.73	-0.69	0.53
5Yr	1.74	-2.30	-1.14	-2.07	0.00	-0.26	-0.24	-0.64	-0.53
10Yr	0.28	0.00	-0.43	-2.13	0.00	-0.24	0.01	-0.45	-0.18
15Yr	-5.43	4.24	6.19	-1.57	0.00	-2.82	-1.95	-0.17	3.78
30Yr	-10.81	-2.40	19.66	11.25	0.00	-5.30	-3.88	2.70	11.04

Table C.1: Calibration errors for 1Y tenor ($\times 10^2$)

Tenor 2Y ($\times 10^2$)	Moneyness								
Expiry	-200bps	-150bps	-100bps	-50bps	ATM	50bps	100bps	150bps	200bps
3Mo	9.06	-11.79	0.17	5.70	0.00	9.27	8.35	-0.29	-9.79
6Mo	-4.22	-2.33	10.68	2.33	0.00	-0.54	0.81	1.31	0.92
1Yr	2.34	-0.51	-1.66	-9.13	0.00	-5.65	-3.84	-0.34	2.65
2Yr	-0.87	0.77	2.09	-4.85	0.00	-2.46	-1.42	-0.40	1.60
3Yr	0.67	-0.80	0.61	-3.84	0.00	-1.21	-1.00	-0.75	0.79
4Yr	0.95	-1.52	0.49	-2.49	0.00	-0.89	-0.76	-0.73	0.58
5Yr	1.67	-2.21	-1.07	-2.10	0.00	-0.37	-0.30	-0.65	-0.42
10Yr	0.26	-0.01	-0.35	-1.95	0.00	-0.22	-0.03	-0.39	-0.16
15Yr	-5.21	4.01	6.03	-1.51	0.00	-2.72	-1.87	-0.23	3.69
30Yr	-9.78	-2.85	18.65	10.71	0.00	-5.09	-3.80	2.37	10.27

Table C.2: Calibration errors for 2Y tenor ($\times 10^2$)

Tenor 3Y ($\times 10^2$)	Moneyness								
Expiry	-200bps	-150bps	-100bps	-50bps	ATM	50bps	100bps	150bps	200bps
3Mo	9.01	-12.13	0.82	6.92	0.00	10.08	9.30	-0.21	-10.61
6Mo	-5.11	-1.91	11.77	2.49	0.00	-0.47	0.91	1.37	1.07
1Yr	2.86	-1.01	-1.90	-9.59	0.00	-5.92	-4.09	-0.36	2.71
2Yr	-0.50	0.31	1.98	-5.00	0.00	-2.52	-1.53	-0.43	1.59
3Yr	0.79	-0.94	0.56	-3.91	0.00	-1.18	-1.03	-0.78	0.78
4Yr	0.84	-1.44	0.64	-2.42	0.00	-0.91	-0.72	-0.66	0.57
5Yr	1.49	-1.91	-0.99	-1.99	0.00	-0.37	-0.24	-0.59	-0.38
10Yr	0.24	0.00	-0.33	-1.88	0.00	-0.24	0.05	-0.38	-0.17
15Yr	-5.03	3.87	5.84	-1.42	0.00	-2.62	-1.84	-0.20	3.56
30Yr	-9.47	-3.26	18.61	10.78	0.00	-5.06	-3.75	2.32	10.19

Table C.3: Calibration errors for 3Y tenor ($\times 10^2$)

Tenor 4Y ($\times 10^2$)	Moneyness								
Expiry	-200bps	-150bps	-100bps	-50bps	ATM	50bps	100bps	150bps	200bps
3Mo	9.06	-12.21	0.87	7.00	0.00	10.20	9.43	-0.22	-10.72
6Mo	-5.34	-2.27	12.61	2.75	0.00	-0.53	0.95	1.51	1.13
1Yr	3.40	-1.51	-2.18	-10.03	0.00	-6.22	-4.25	-0.47	2.80
2Yr	-0.29	0.06	1.93	-5.09	0.00	-2.63	-1.50	-0.45	1.55
3Yr	0.75	-0.90	0.61	-3.94	0.00	-1.17	-0.96	-0.81	0.78
4Yr	0.69	-1.15	0.63	-2.46	0.00	-0.86	-0.68	-0.67	0.59
5Yr	1.29	-1.60	-0.86	-1.87	0.00	-0.28	-0.19	-0.47	-0.36
10Yr	0.31	-0.06	-0.45	-2.06	0.00	-0.25	-0.04	-0.45	-0.17
15Yr	-4.59	3.42	5.49	-1.25	0.00	-2.51	-1.69	-0.24	3.33
30Yr	-9.00	-3.61	18.24	10.61	0.00	-5.06	-3.83	2.23	10.02

Table C.4: Calibration errors for 4Y tenor ($\times 10^2$)

Tenor 5Y ($\times 10^2$)	Moneyness								
Expiry	-200bps	-150bps	-100bps	-50bps	ATM	50bps	100bps	150bps	200bps
3Mo	9.64	-13.00	0.93	7.48	0.00	10.89	10.01	-0.19	-11.45
6Mo	-5.12	-2.59	12.61	2.78	0.00	-0.54	0.90	1.56	1.11
1Yr	3.72	-1.86	-2.28	-10.18	0.00	-6.31	-4.26	-0.48	2.75
2Yr	-0.28	0.04	1.92	-5.14	0.00	-2.61	-1.56	-0.51	1.63
3Yr	0.56	-0.68	0.72	-3.88	0.00	-1.13	-0.98	-0.76	0.81
4Yr	0.47	-0.85	0.67	-2.31	0.00	-0.81	-0.67	-0.59	0.60
5Yr	1.22	-1.47	-0.87	-1.91	0.00	-0.28	-0.25	-0.45	-0.34
10Yr	0.27	0.00	-0.43	-1.97	0.00	-0.17	-0.02	-0.40	-0.19
15Yr	-4.52	3.30	5.51	-1.39	0.00	-2.60	-1.78	-0.31	3.44
30Yr	-8.50	-4.06	17.98	10.49	0.00	-4.99	-3.75	2.09	9.80

Table C.5: Calibration errors for 5Y tenor ($\times 10^2$)

Tenor 10Y ($\times 10^2$)	Moneyness								
Expiry	-200bps	-150bps	-100bps	-50bps	ATM	50bps	100bps	150bps	200bps
3Mo	8.51	-11.69	1.19	7.44	0.00	10.15	9.58	-0.13	-10.71
6Mo	-5.93	-1.85	13.19	2.68	0.00	-0.60	0.95	1.57	1.27
1Yr	3.04	-1.20	-1.94	-9.77	0.00	-6.00	-4.16	-0.41	2.76
2Yr	-0.95	0.89	2.14	-5.09	0.00	-2.62	-1.55	-0.36	1.67
3Yr	-0.14	0.26	0.97	-3.83	0.00	-1.15	-0.93	-0.61	0.88
4Yr	-0.03	-0.15	0.92	-2.37	0.00	-0.84	-0.60	-0.49	0.66
5Yr	0.97	-1.13	-0.64	-1.86	0.00	-0.35	-0.16	-0.36	-0.28
10Yr	0.45	-0.29	-0.51	-2.02	0.00	-0.22	-0.02	-0.48	-0.25
15Yr	-3.87	2.38	5.36	-1.25	0.00	-2.67	-1.83	-0.34	3.36
30Yr	-5.77	-6.08	15.96	9.62	0.00	-4.68	-3.61	1.46	8.35

Table C.6: Calibration errors for 10Y tenor ($\times 10^2$)

Tenor 15Y ($\times 10^2$)	Moneyness								
Expiry	-200bps	-150bps	-100bps	-50bps	ATM	50bps	100bps	150bps	200bps
3Mo	8.41	-11.86	1.70	8.21	0.00	10.74	10.14	-0.12	-11.18
6Mo	-6.46	-1.23	13.34	2.68	0.00	-0.59	0.97	1.61	1.30
1yr	2.79	-0.97	-1.81	-9.58	0.00	-5.92	-4.02	-0.45	2.77
2Yr	-0.98	0.96	2.03	-4.71	0.00	-2.40	-1.39	-0.30	1.52
3Yr	-0.11	0.22	0.87	-3.54	0.00	-1.12	-0.82	-0.59	0.82
4Yr	0.05	-0.25	0.79	-2.17	0.00	-0.88	-0.60	-0.45	0.63
5Yr	1.11	-1.31	-0.77	-1.89	0.00	-0.36	-0.21	-0.39	-0.30
10Yr	0.67	-0.69	-0.62	-1.88	0.00	-0.25	-0.03	-0.51	-0.34
15Yr	-3.11	1.36	5.13	-1.11	0.00	-2.55	-1.82	-0.46	3.23
30Yr	-5.15	-7.91	16.75	10.30	0.00	-5.02	-3.93	1.58	8.98

Table C.7: Calibration errors for 15Y tenor ($\times 10^2$)

Tenor 30Y ($\times 10^2$)	Moneyness								
Expiry	-200bps	-150bps	-100bps	-50bps	ATM	50bps	100bps	150bps	200bps
3Mo	8.61	-12.11	1.66	8.24	0.00	10.85	10.14	-0.08	-11.29
6Mo	-6.15	-1.57	13.21	2.71	0.00	-0.57	0.97	1.53	1.31
1Yr	3.11	-1.30	-2.01	-9.55	0.00	-5.97	-4.05	-0.39	2.68
2Yr	-0.74	0.61	2.08	-4.95	0.00	-2.50	-1.44	-0.43	1.60
3Yr	0.17	-0.13	0.70	-3.49	0.00	-1.14	-0.83	-0.64	0.78
4Yr	0.35	-0.67	0.68	-2.21	0.00	-0.81	-0.64	-0.50	0.57
5Yr	1.25	-1.59	-0.84	-1.86	0.00	-0.33	-0.28	-0.48	-0.34
10Yr	0.95	-1.11	-0.80	-1.99	0.00	-0.23	-0.10	-0.57	-0.49
15Yr	-2.43	0.55	4.78	-1.17	0.00	-2.54	-1.88	-0.56	3.13
30Yr	-3.63	-9.88	16.40	10.44	0.00	-5.00	-3.99	1.34	8.72

Table C.8: Calibration errors for 30Y tenor ($\times 10^2$)

Appendix D

SABR Greeks

Within the SABR model, the primary concerns of traders are the sensitivities of the model to changes its parameters; the volatility α; the curvature ρ, and the skewness ν. The model's sensitivity to the forward swap rate is also clearly of importance (Hagan et al., 2002).

First let, $V_{call} = BS(f, K, \sigma_B(K, f), t_{ex})$. Then Hagan et al. (2002) define the following greeks through differentiation of equation 2.4:

$$
\begin{aligned}
\text{Vega} = \frac{\partial V_{call}}{\partial \alpha} &= \frac{\partial BS}{\partial \sigma_B} \cdot \frac{\partial \sigma_B(K, f; \alpha, \beta, \rho, \nu)}{\partial \alpha} \\
&\approx \frac{\partial BS}{\partial \sigma_B} \cdot \frac{\sigma_B(K, f)}{\sigma_B(f, f)}, && \text{(D.1)} \\
\text{Vanna} = \frac{\partial V_{call}}{\partial \rho} &= \frac{\partial BS}{\partial \sigma_B} \cdot \frac{\partial \sigma_B(K, f; \alpha, \beta, \rho, \nu)}{\partial \rho}, && \text{(D.2)} \\
\text{Volga} = \frac{\partial V_{call}}{\partial \nu} &= \frac{\partial BS}{\partial \sigma_B} \cdot \frac{\partial \sigma_B(K, f; \alpha, \beta, \rho, \nu)}{\partial \nu}, && \text{(D.3)} \\
\text{Delta} = \frac{\partial V_{call}}{\partial f} &= \frac{\partial BS}{\partial f} + \frac{\partial BS}{\partial \sigma_B} \cdot \frac{\partial \sigma_B(K, f; \alpha, \beta, \rho, \nu)}{\partial f}. && \text{(D.4)}
\end{aligned}
$$

Vega is the sensitivity of the price to volatility; Vanna is the sensitivity of the price to a change in skew; Volga is the sensitivity of the price to a change in curvature of the volatility smile; and Delta is the sensitivity of the price to the forward rate.

Note that an approximation is applied to ease the calculation of vega and all other derivatives are calculated numerically using the relevant method outlined in appendix F.

For each tenor of swaption, a surface can be formulated for each of the above greeks. Returning to the example of the 5 year tenor, such surfaces can be seen below.

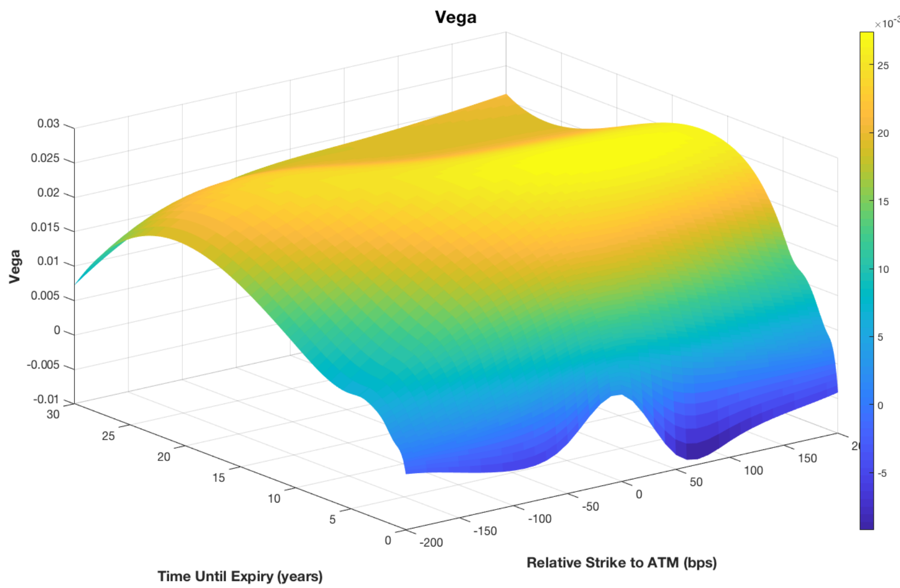

Figure D.1: Vega surface for 5Y tenor

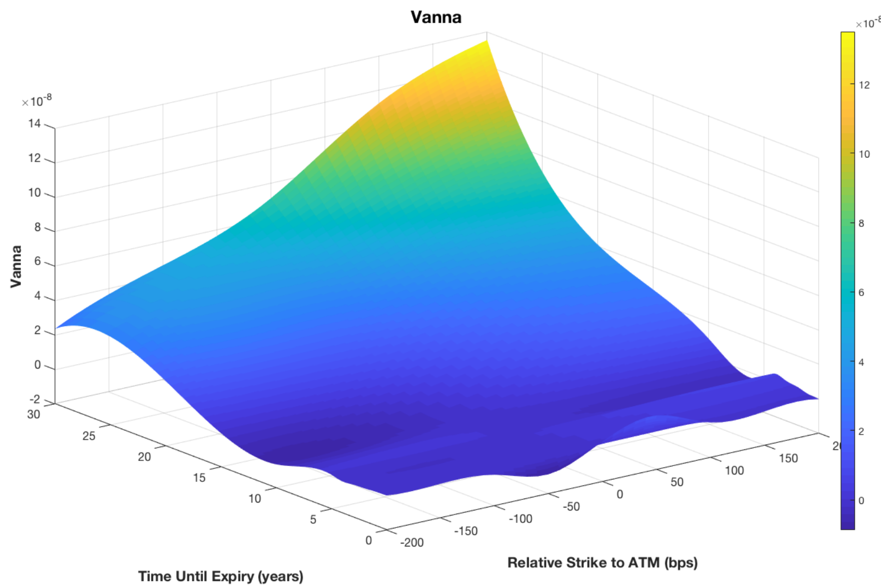

Figure D.2: Vanna surface for 5Y tenor

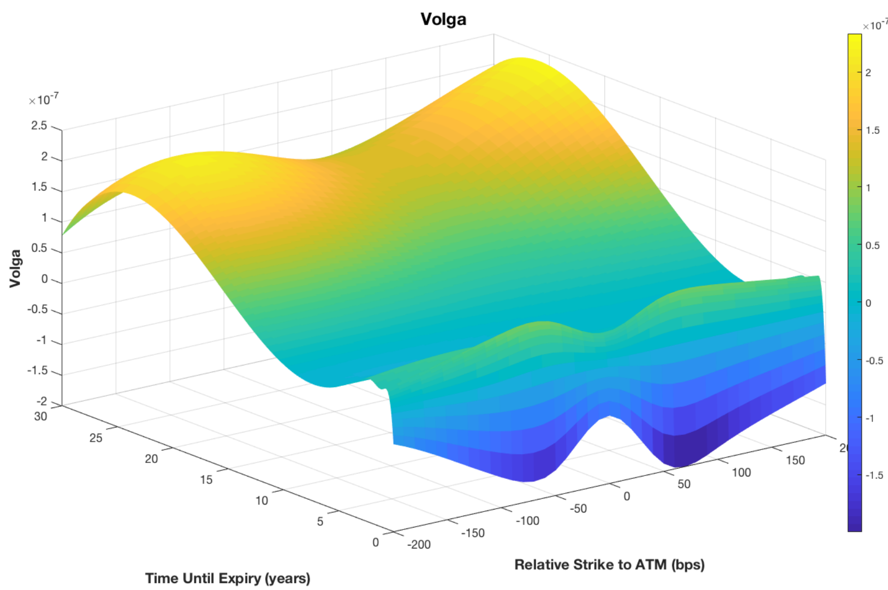

Figure D.3: Volga surface for 5Y tenor

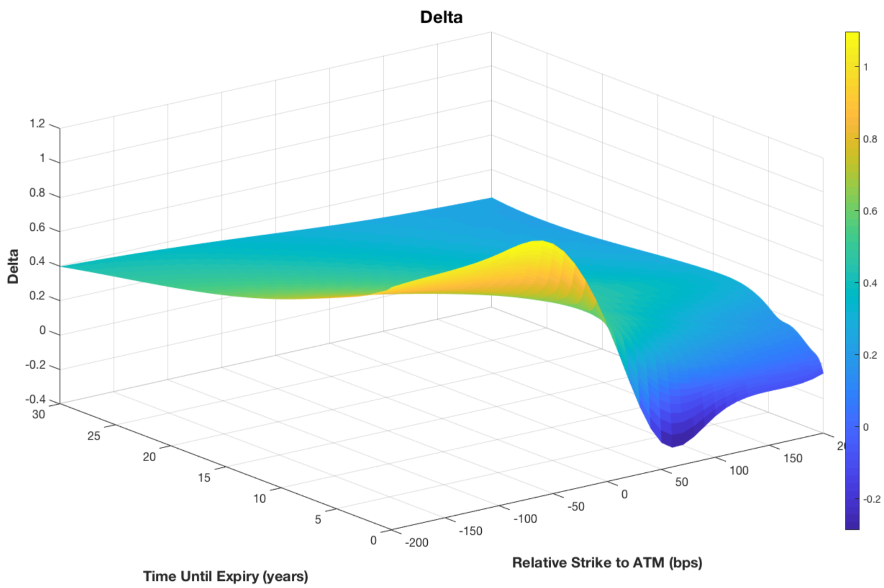

Figure D.4: Delta surface for 5Y tenor

Appendix E

SABR Derivation

The following derivation should be considered a rough outline of the derivation of the SABR model adapted from Hagan et al. (2002) to aid the intuition of the reader. The full and rigorous derivation can be found in appendix B of Hagan et al. (2002).

The derivation is based on volatility expansions of $\hat{\alpha}$ and ν. Considering this and taking the generalised form, the equations 2.1-2.3 can be expressed as,

$$d\hat{F} = \epsilon\hat{\alpha}C(\hat{F})dW_1, \quad \hat{F}(0) = f, \tag{E.1}$$

$$d\hat{\alpha} = \epsilon\nu\hat{\alpha}dW_2, \quad \hat{\alpha}(0) = \alpha, \tag{E.2}$$

$$\rho dt = dW_1 dW_2. \tag{E.3}$$

Let the time of maturity be denoted by T. Then the probability density is given by,

$$p(t, f, \alpha; T, F, A)dFdA = \mathbb{P}\{F < \hat{F}(T) < F+dF, A < \hat{\alpha}(T) < A+dA \mid \hat{F}(t) = f, \hat{\alpha}(t) = \alpha\}, \tag{E.4}$$

and so, at maturity is defined as,

$$p(t, f, \alpha; T, F, A) = \delta(F - f)\delta(A - \alpha) + \int_t^T p_T(t, f, \alpha; T, F, A)dT, \tag{E.5}$$

where,

$$p_T = \frac{1}{2}\epsilon^2 A^2 \frac{\partial^2}{\partial F^2}C^2(F)p + \epsilon^2\rho\nu\frac{\partial^2}{\partial F\partial A}A^2C^2(F)p + \frac{1}{2}\epsilon^2\nu^2\frac{\partial^2}{\partial A^2}A^2p. \tag{E.6}$$

Now let the value of a European call option be:

$$\begin{aligned}
V(t,f,\alpha) &= \mathbb{E}([\hat{F}(T)-K]^+ \mid \hat{F}(t)=f, \hat{\alpha}(t)=\alpha) \\
&= \int_{-\infty}^{\infty}\int_{K}^{\infty}(F-K)p(t,f,\alpha;T,F,A)dFdA \\
&= [f-K]^+ + \int_t^T \int_{-\infty}^{\infty}\int_{K}^{\infty}(F-K)p_T(t,f,\alpha;T,F,A)dT \\
&= [f-K]^+ + \frac{\epsilon^2}{2}\int_t^T \int_{-\infty}^{\infty}\int_{K}^{\infty} A^2(F-K)\frac{\partial^2}{\partial F^2}C^2(F)pdFdAdT \\
&= [f-K]^+ + \frac{\epsilon^2 C^2(K)}{2}\int_t^T \int_{-\infty}^{\infty} A^2 p(t,f,\alpha;T,F,A)dAdT \\
&= [f-K]^+ + \frac{\epsilon^2 C^2(K)}{2}\int_t^{\tau} P(\tau,f,\alpha;K)d\tau, \qquad \text{(E.7)}
\end{aligned}$$

where,

$$P(\tau,f,\alpha;K) = \int_{-\infty}^{\infty} A^2 p(t,f,\alpha;T,F,A)dA, \qquad \text{(E.8)}$$

and

$$\begin{aligned}
&P_\tau = \frac{1}{2}\epsilon^2\alpha^2C^2(f)\frac{\partial^2 P}{\partial f^2} + \epsilon^2\rho\nu\frac{\partial^2 P}{\partial f\partial\alpha}\alpha^2C^2(f) + \frac{1}{2}\epsilon^2\nu^2\frac{\partial^2 P}{\partial\alpha^2}\alpha^2 \text{ for } \tau > 0 \\
&P = \alpha^2\delta(f-K) \text{ for } \tau = 0, \qquad \text{(E.9)}
\end{aligned}$$

with $\tau = T - t$. While the above PDE could be solved numerically from this point, to obtain the SABR model and more efficient computation we continue with perturbation expansions.

Singular Perturbation Expansion

Using a basic perturbation expansion results in a Gaussian density of the form,

$$P = \frac{\alpha}{\sqrt{2\pi\epsilon^2C^2(K)\tau}}e^{-\frac{(f-K)^2}{2\epsilon^2\alpha^2C^2(K)\tau}}\{1+\ldots\}. \qquad \text{(E.10)}$$

However, this form is problematic as the "$+\ldots$" term becomes significant once $C(f)$ and $C(K)$ differ by too much (Hagan et al., 2002). This would clearly cause problems when evaluating far OTM swaptions. To remedy this, the series is reformulated as,

$$P = \frac{\alpha}{\sqrt{2\pi\epsilon^2 C^2(K)\tau}} e^{-\frac{(f-K)^2}{2\epsilon^2\alpha^2 C^2(K)\tau}\{1+\ldots\}}, \tag{E.11}$$

enabling the expansion of the exponent.

Following this expansion, the value of the European call option can be expressed as,

$$V(t,f,\alpha) = [f-K]^+ + \frac{|f-K|}{4\sqrt{\pi}} \int_{\frac{x^2}{2\tau}-\epsilon^2\theta}^{\infty} \frac{e^{-q}}{q^{3/2}} dq, \tag{E.12}$$

where,

$$\begin{aligned}
x &= \frac{1}{\epsilon\nu} \log\left(\frac{\sqrt{1-2\epsilon\rho\nu z+\epsilon^2\nu^2 z^2}-\rho+\epsilon\nu z}{1-\rho}\right), \\
z &= \frac{1}{\epsilon\alpha}\int_K^f \frac{df'}{C(f')}, \\
\epsilon^2\theta &= \log\left(\frac{\epsilon\alpha z}{f-K}\sqrt{B(0)B(\epsilon\alpha z)}\right) + \log\left(\frac{x I^{1/2}(\epsilon\nu z)}{z}\right) + \frac{1}{4}\epsilon^2\rho\nu\alpha b_1 z^2, \\
I(q) &= \sqrt{(1-2\rho q+q^2)}, \\
b_1 &= \frac{B'(\epsilon\alpha z_0)}{B(\epsilon\alpha z_0)}, \\
B(\epsilon\alpha z) &= C(f).
\end{aligned}$$

Equivalent Normal Volatility

If the above derivation is repeated using the normal model with constant σ_N, $C(f)=1$ and $\nu=0$ as,

$$d\hat{F} = \sigma_N dW, \quad \hat{F}(0) = f, \tag{E.13}$$

then the option value is given by:

$$V(t,f) = [f-K]^+ + \frac{|f-K|}{4\sqrt{\pi}} \int_{\frac{(f-K)^2}{2\sigma_N^2\tau}}^{\infty} \frac{e^{-q}}{q^{3/2}} dq. \tag{E.14}$$

Integrating gives,

$$V(t,f) = (f-K)\Phi\left(\frac{f-K}{\sigma_N\sqrt{\tau}}\right) + \sigma_N\sqrt{\tau}\phi\left(\frac{f-K}{\sigma_N\sqrt{\tau}}\right), \tag{E.15}$$

where, Φ is the standard normal cumulative distribution and ϕ is the standard normal density function. The option price under both the normal and SABR model will then be equal if and only if,

$$\sigma_N = \frac{f-K}{x}\left\{1 + \epsilon^2\frac{\theta}{x^2}\tau + \dots\right\} \tag{E.16}$$

up to $\mathcal{O}(\epsilon^2)$. Substituting in, we achieve:

$$\begin{aligned}\sigma_N(K) = &\frac{\epsilon\alpha(f-K)}{\int_K^f \frac{df'}{C(f')}} \times \left(\frac{z}{\hat{x}(z)}\right) \times \\ &\left\{1 + \left[\frac{2\gamma_2-\gamma_1^2}{24}\alpha^2C^2(\sqrt{fK}) + \frac{1}{4}\rho\nu\alpha\gamma_1C(\sqrt{fK}) + \frac{2-3\rho^2}{24}\nu^2\right]\epsilon^2\tau + \dots\right\},\end{aligned} \tag{E.17}$$

with,

$$\begin{aligned}\gamma_1 &= \frac{C'(\sqrt{fK})}{C(\sqrt{fK})}, \\ \gamma_2 &= \frac{C''(\sqrt{fK})}{C(\sqrt{fK})}, \\ z &= \frac{\nu(f-K)}{\alpha C(\sqrt{fK})}, \end{aligned} \tag{E.18}$$

$$\hat{x}(z) = \log\left(\frac{\sqrt{1-2\rho z+z^2}-\rho+z}{1-\rho}\right). \tag{E.19}$$

Equivalent Black Volatility

Consider the model again with $C(f) = f$ and $\nu = 0$ so that,

$$d\hat{F} = \epsilon\sigma_B\hat{F}dW, \quad \hat{F}(0) = f. \tag{E.20}$$

Applying these changes to equation E.16 and results in,

$$\sigma_N(K) = \frac{\epsilon\sigma_B(f-K)}{\log\frac{f}{K}}\left\{1 + \frac{1}{24}\epsilon^2\sigma_B^2\tau + \dots\right\}. \tag{E.21}$$

Solving this equation for Black's implied volatility yields,

$$\sigma_B(K) = \frac{\alpha \log(\frac{f}{K})}{\int_K^f \frac{df'}{C(f')}} \times \left(\frac{z}{\hat{x}(z)}\right) \times$$
$$\left\{1 + \left[\frac{2\gamma_2 - \gamma_1^2 + \frac{1}{fK}}{24}\alpha^2 C^2(\sqrt{fK}) + \frac{1}{4}\rho\nu\alpha\gamma_1 C(\sqrt{fK}) + \frac{2-3\rho^2}{24}\nu^2\right]\epsilon^2\tau + \dots\right\}. \tag{E.22}$$

Stochastic β Model

Finally, consider the model with $C(f) = f^\beta$ such that,

$$d\hat{F} = \epsilon\sigma_N \hat{F}^\beta dW, \quad \hat{F}(0) = f. \tag{E.23}$$

Also consider the following approximations:

$$f - K = \sqrt{fK}\log(f/K)\left\{1 + \frac{1}{24}\log^2(f/K) + \frac{1}{1920}\log^4(f/K) + \dots\right\},$$
$$f^{(1-\beta)} - K^{(1-\beta)} = (1-\beta)(fK)^{\frac{(1-\beta)}{2}}\log(f/K)\times$$
$$\left\{1 + \frac{(1-\beta)^2}{24}\log^2(f/K) + \frac{(1-\beta)^4}{1920}\log^4(f/K) + \dots\right\}.$$

Substituting in $C(f) = f^\beta$ and using the above approximations yields,

$$\sigma_N(K) = \epsilon\alpha(fK)^{\beta/2}\frac{1 + \frac{1}{24}\log^2(f/K) + \frac{1}{1920}\log^4(f/K) + \dots}{1 + \frac{(1-\beta)^2}{24}\log^2(f/K) + \frac{(1-\beta)^2}{1920}\log^4(f/K) + \dots}$$
$$\times \left(\frac{z}{\hat{x}(z)}\right)$$
$$\times \left\{1 + \left[\frac{-\beta(2-\beta)\alpha^2}{24(fK)^{1-\beta}} + \frac{\rho\alpha\nu\beta}{4(fK)^{(1-\beta)/2}} + \frac{2-3\rho^2}{24}\nu^2\right]\epsilon^2\tau + \dots\right\}, \tag{E.24}$$

where z and $x(z)$ are as defined in equations E.18 and E.19.

Setting $\epsilon = 1$ results in,

$$\begin{aligned}\sigma_B(K,f) =& \frac{\alpha}{(fK)^{(1-\beta)/2}\left\{1+\frac{(1-\beta)^2}{24}\log^2(\frac{f}{K})+\frac{(1-\beta)^4}{1920}\log^4(\frac{f}{K})+\dots\right\}}\\ &\times\left(\frac{z}{x(z)}\right)\\ &\times\left\{1+\left[\frac{(1-\beta)^2}{24}\frac{\alpha^2}{(fK)^{(1-\beta)}}+\frac{1}{4}\frac{\rho\beta\nu\alpha}{(fK)^{(1-\beta)/2}}+\frac{2-3\rho^2}{24}\nu^2\right]T+\dots\right\},\end{aligned} \tag{E.25}$$

where,

$$\begin{aligned} z &= \frac{\nu}{\alpha}(fK)^{(1-\beta)/2}\log(\frac{f}{K}),\\ x(z) &= \log\left\{\frac{\sqrt{1-2\rho z+z^2}+z+\rho}{1-\rho}\right\}.\end{aligned}$$

The above is equal to equation 2.4 and so the derivation is complete.

Appendix F

Numerical Methods

First order derivatives were based on the symmetric difference quotient:

$$f'(x) = \frac{f(x+h) - f(x-h)}{2h}, \tag{F.1}$$

and calculated as,

$$f'(x_i) = \frac{f(x_{i+1}) - f(x_{i-1})}{2h}, \tag{F.2}$$

where h is the step size used in the discretisation.

As the implied volatility surface is assumed to be relatively smooth, and thus differentiable, the numerical approximation of the symmetric derivative generally does a better job than the other basic approximations (Lax, Terrell, 2013). Flat extrapolation was used for the boundary points as in Gatarek & Jablecki (2017).

The second order derivatives were similarly based on the second symmetric derivative:

$$f'(x) = \frac{f(x+h) - 2f(x) + f(x-h)}{h^2}, \tag{F.3}$$

and calculated as,

$$f'(x_i) = \frac{f(x_{i+1}) - 2f(x_i) + f(x_{i-1})}{h^2}. \tag{F.4}$$

Note that other methods of approximating the derivatives were tested and yielded highly similar results.